INSTITUTE OF PHYSICS PUBLISHING JOURNAL OF PHYSICS A: MATHEMATICAL AND GENERAL

J. Phys. A: Math. Gen. **39** (2006) 10057–10076 doi:10.1088/0305-4470/39/32/S08

A Krein space related perturbation theory for MHD α^2-dynamos and resonant unfolding of diabolical points

Uwe Günther[1] **and Oleg N Kirillov**[2]

[1] Research Center Rossendorf, PO Box 510119, D-01314 Dresden, Germany
[2] Institute of Mechanics, Moscow State Lomonosov University, Michurinskii pr. 1, 119192 Moscow, Russia

E-mail: u.guenther@fz-rossendorf.de and kirillov@imec.msu.ru

Received 3 February 2006, in final form 7 March 2006
Published 26 July 2006
Online at stacks.iop.org/JPhysA/39/10057

Abstract

The spectrum of the spherically symmetric α^2-dynamo is studied in the case of idealized boundary conditions. Starting from the exact analytical solutions of models with constant α-profiles, a perturbation theory and a Galerkin technique are developed in a Krein space approach. With the help of these tools, a very pronounced α-resonance pattern is found in the deformations of the spectral mesh as well as in the unfolding of the diabolical points located at the nodes of this mesh. Non-oscillatory as well as oscillatory dynamo regimes are obtained. An estimation technique is developed for obtaining the critical α-profiles at which the eigenvalues enter the right spectral half-plane with non-vanishing imaginary components (at which overcritical oscillatory dynamo regimes form). Finally, Fréchet derivative (gradient) based methods are developed, suitable for further numerical investigations of Krein space related setups such as MHD α^2-dynamos or models of $\mathcal{PT}$-symmetric quantum mechanics.

PACS numbers: 02.30.Tb, 91.25.Cw, 11.30.Er, 02.40.Xx
Mathematics Subject Classification: 47B50, 46C20, 47A11, 32S05

1. Introduction

The mean field α^2-dynamo of magnetohydrodynamics (MHD) [1–3] plays a similar paradigmatic role in MHD dynamo theory as the harmonic oscillator in quantum mechanics. In its kinematic regime, this dynamo is described by a *linear* induction equation for the magnetic field. For spherically symmetric α-profiles $\alpha(r)$, the vector of the magnetic field can be decomposed into poloidal and toroidal components and expanded in spherical harmonics.

After additional time separation, the induction equation reduces to a set of l-decoupled boundary eigenvalue problems [2, 4, 5]

$$\mathfrak{A}_\alpha \mathfrak{u} = \lambda \mathfrak{u}, \qquad \mathfrak{u}(r \searrow 0) = \mathfrak{u}(1) = 0 \tag{1}$$

for matrix differential operators

$$\mathfrak{A}_\alpha := \begin{pmatrix} -A_l & \alpha(r) \\ A_{l,\alpha} & -A_l \end{pmatrix}, \tag{2}$$

with [4, 5]

$$\begin{aligned} A_l &:= -\partial_r^2 + \frac{l(l+1)}{r^2}, \\ A_{l,\alpha} &:= -\partial_r \alpha(r) \partial_r + \alpha(r) \frac{l(l+1)}{r^2} = \alpha(r) A_l - \alpha'(r) \partial_r. \end{aligned} \tag{3}$$

The boundary conditions in (1) are idealized ones and formally coincide with those for dynamos in a high-conductivity limit of the dynamo maintaining fluid/plasma [6]. We will restrict our subsequent considerations to this case and assume a domain

$$\mathcal{D}(\mathfrak{A}_\alpha) = \{\mathfrak{u} \in \tilde{\mathcal{H}} = L_2(0,1) \oplus L_2(0,1) | \mathfrak{u}(r \searrow 0) = \mathfrak{u}(1) = 0\} \tag{4}$$

in the Hilbert space $(\tilde{\mathcal{H}}, (.,.))$. The α-profile $\alpha(r)$ is a smooth real function $C^2(0,1) \ni \alpha(r) : (0,1) \to \mathbb{R}$ and plays the role of the potential in dynamo models.

Due to the fundamental symmetry of its differential expression [4, 5],

$$\mathfrak{A}_\alpha = J \mathfrak{A}_\alpha^\dagger J, \qquad J = \begin{pmatrix} 0 & I \\ I & 0 \end{pmatrix}, \tag{5}$$

the operator $\mathfrak{A}_\alpha$ is a symmetric operator in a Krein space $(\mathcal{K}, [.,.])$ [7–11] with an indefinite inner product $[.,.] = (J.,.)$ and for the chosen domain (4) it is also self-adjoint in this space

$$[\mathfrak{A}_\alpha x, y] = [x, \mathfrak{A}_\alpha y], \qquad x, y \in \mathcal{K}. \tag{6}$$

Below we analyse the spectrum of the operator $\mathfrak{A}_\alpha$ in the vicinity of constant α-profiles—analytically with the help of a perturbation theory as well as numerically with a Galerkin approximation. We obtain a pronounced α-resonance pattern in the occurring deformations of the spectral mesh as well as in the unfolding of the semi-simple (diabolical [12]) degeneration points which form the nodes of this mesh. Additionally, we develop an estimation technique which allows us to obtain the critical α-profiles at which the eigenvalues enter the right spectral half-plane with non-vanishing imaginary components (at which overcritical oscillatory dynamo regimes form). We demonstrate this technique explicitly for $(l = 0)$-models, where it leads to a bound on the Fourier components of the α-profile.

2. Basis properties of the eigenfunctions in the case of constant α-profiles

For constant α-profiles $\alpha(r) \equiv \alpha_0 = \text{const}$, $r \in [0,1)$, the operator matrix (2) takes the simple form

$$\mathfrak{A}_{\alpha_0} = \begin{pmatrix} -1 & 0 \\ \alpha_0 & -1 \end{pmatrix} \otimes A_l + \begin{pmatrix} 0 & \alpha_0 \\ 0 & 0 \end{pmatrix} \otimes I, \tag{7}$$

so that the two-component eigenfunctions $\mathfrak{u}(r)$ can be easily derived with the help of an ansatz

$$\mathfrak{u}_n(r) = \begin{pmatrix} C_1 \\ C_2 \end{pmatrix} \otimes u_n(r) \in \mathbb{C}^2 \otimes L_2(0,1), \tag{8}$$

where $C_1, C_2 \in \mathbb{C}$ are constants to be determined and u_n are the eigenfunctions of the operator A_l

$$A_l u_n = \rho_n u_n, \qquad u_n(r \searrow 0) = u_n(r = 1) = 0. \tag{9}$$

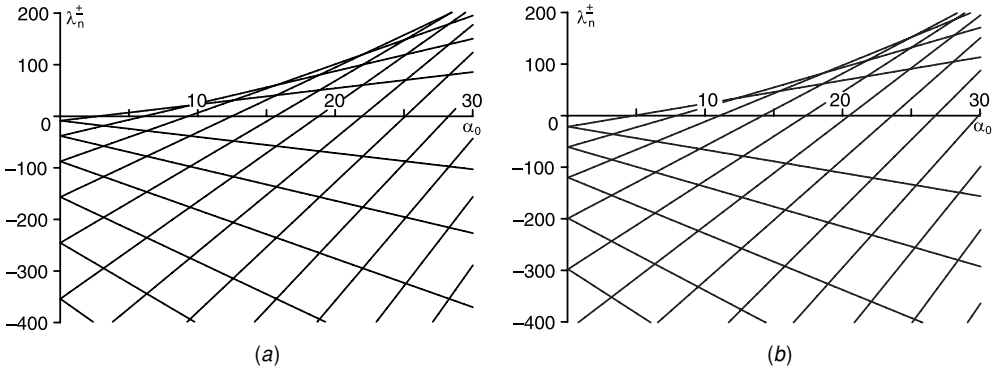

Figure 1. Eigenvalues $\lambda_n^{\pm}$ ($\alpha_0 \geqslant 0$) for $l = 0$ (*a*) and $l = 1$ (*b*). The spectral branches intersect at semi-simple degeneration points (diabolical points) of algebraic and geometric multiplicity 2.

These eigenfunctions u_n are Riccati–Bessel functions [13]

$$u_n(r) = N_n r^{1/2} J_{l+\frac{1}{2}}(\sqrt{\rho_n} r), \qquad N_n := \frac{\sqrt{2}}{J_{l+\frac{3}{2}}(\sqrt{\rho_n})} \tag{10}$$

and we orthonormalized them as[3]

$$(u_m, u_n) = \delta_{mn}, \qquad \|u_n\| = 1. \tag{11}$$

Accordingly, the spectrum of the operator A_l consists of simple positive-definite eigenvalues $\rho_n > 0$—the squares of Bessel function zeros

$$J_{l+\frac{1}{2}}(\sqrt{\rho_n}) = 0, \qquad 0 < \sqrt{\rho_1} < \sqrt{\rho_2} < \cdots. \tag{12}$$

Spectrum and eigenvectors of the operator matrix $\mathfrak{A}_{\alpha_0}$ follow from (7) and (8) as

$$\lambda_n^{\pm} = \lambda_n^{\pm}(\alpha_0) = -\rho_n \pm \alpha_0 \sqrt{\rho_n} \in \mathbb{R}, \qquad n \in \mathbb{Z}^+, \tag{13}$$

and

$$\mathfrak{u}_n^{\pm} = \begin{pmatrix} 1 \\ \pm\sqrt{\rho_n} \end{pmatrix} u_n \in \mathbb{R}^2 \otimes L_2(0, 1), \tag{14}$$

and correspond to Krein space states of positive and negative types

$$\left[\mathfrak{u}_m^{\pm}, \mathfrak{u}_n^{\pm}\right] = \pm 2\sqrt{\rho_n}\delta_{mn}, \qquad \left[\mathfrak{u}_m^{\pm}, \mathfrak{u}_n^{\mp}\right] = 0, \qquad \mathfrak{u}_n^{\pm} \in \mathcal{K}_{\pm} \subset \mathcal{K}. \tag{15}$$

The branches $\lambda_n^{\pm}$ of the spectrum are real-valued linear functions of the parameter α_0 with slopes $\pm\sqrt{\rho_n}$ and form a mesh-like structure in the $(\alpha_0, \operatorname{Re}\lambda)$-plane, as depicted in figure 1. In order to calculate the intersection points of the spectral branches (the nodes of the spectral mesh), we introduce the following convenient notation:

$$\lambda_n^{\varepsilon} = -\rho_n + \varepsilon\alpha_0\sqrt{\rho_n}, \qquad \varepsilon = \pm, \qquad \mathfrak{u}_n^{\varepsilon} = \begin{pmatrix} 1 \\ \varepsilon\sqrt{\rho_n} \end{pmatrix} u_n, \tag{16}$$

which allows us to treat positive and negative Krein space states in a unified way.

Two branches λ_m^{δ} and λ_n^{ε} with $n \neq m$ intersect at a point $\left(\alpha_0^{\nu}, \lambda_0^{\nu}\right)$ when

$$\begin{aligned} &\lambda_n^{\varepsilon} = \lambda_m^{\delta}, && -\rho_n + \varepsilon\alpha_0\sqrt{\rho_n} = -\rho_m + \delta\alpha_0\sqrt{\rho_m}, \\ &\alpha_0 = \frac{\rho_n - \rho_m}{\varepsilon\sqrt{\rho_n} - \delta\sqrt{\rho_m}}, && \alpha_0^{\nu} := \alpha_0 = \varepsilon\sqrt{\rho_n} + \delta\sqrt{\rho_m}, \end{aligned} \tag{17}$$

[3] See appendix A for Riccati–Bessel functions and related orthogonality conditions.

and hence

$$\lambda_n^{\varepsilon} = \lambda_m^{\delta} = \lambda_0^{\nu} := \varepsilon\delta\sqrt{\rho_n\rho_m}. \tag{18}$$

Equations (17) and (18) imply that spectral branches of different types $\delta \neq \varepsilon$ intersect for both signs of α_0 at $\lambda_0^{\nu} < 0$. In contrast, intersections at $\lambda_0^{\nu} > 0$ are induced by spectral branches of positive type when $\alpha_0 > 0$ and by spectral branches of negative type when $\alpha_0 < 0$.

According to equation (14), the double eigenvalue λ_0^{ν} possesses the two distinct eigenvectors $\mathfrak{u}_n^{\varepsilon}$ and $\mathfrak{u}_m^{\delta}$:

$$\mathfrak{u}_n^{\varepsilon} = \begin{pmatrix} 1 \\ \varepsilon\sqrt{\rho_n} \end{pmatrix} u_n, \qquad \mathfrak{u}_m^{\delta} = \begin{pmatrix} 1 \\ \delta\sqrt{\rho_m} \end{pmatrix} u_m. \tag{19}$$

Consequently, the intersection points given by (17) correspond to double eigenvalues (18) with two linearly independent eigenvectors (19), i.e. they are semi-simple eigenvalues or diabolical points [12, 14–16] of algebraic and geometric multiplicity 2.

3. Unfolding diabolical points by perturbations of the α-profile

Let us assume that the operator $\mathfrak{A}_{\alpha_0^{\nu}}$ for $\alpha_0 = \alpha_0^{\nu}$ has a semi-simple double eigenvalue λ_0^{ν} with eigenvectors $\mathfrak{u}_n^{\varepsilon}$ and $\mathfrak{u}_m^{\delta}$ determined by equations (18) and (19). Consider a perturbation of the α-profile of the form

$$\alpha(r) = \alpha_0^{\nu} + \Delta\alpha(r) = \alpha_0^{\nu} + \epsilon\varphi(r). \tag{20}$$

Then, the perturbed operator is given by

$$\mathfrak{A}_{\alpha} = \mathfrak{A}_{\alpha_0^{\nu}} + \epsilon \begin{pmatrix} 0 & \varphi(r) \\ \varphi(r)A_l - \varphi'(r)\partial_r & 0 \end{pmatrix} =: \mathfrak{A}_{\alpha_0^{\nu}} + \epsilon\mathfrak{B} \tag{21}$$

and the eigenvalue problem can be expanded in terms of the small parameter ϵ [14–16] as

$$\big(\mathfrak{A}_{\alpha_0^{\nu}} + \epsilon\mathfrak{B}\big)\big(\mathfrak{u}_0^{\nu} + \epsilon\mathfrak{u}_1 + \cdots\big) = \big(\lambda_0^{\nu} + \epsilon\lambda_1 + \cdots\big)\big(\mathfrak{u}_0^{\nu} + \epsilon\mathfrak{u}_1 + \cdots\big). \tag{22}$$

Here, $\mathfrak{u}_0^{\nu}$ is an eigenvector of the unperturbed operator $\mathfrak{A}_{\alpha_0^{\nu}}$, corresponds to the eigenvalue λ_0^{ν} and, hence, has to be a linear combination of $\mathfrak{u}_n^{\varepsilon}$ and $\mathfrak{u}_m^{\delta}$:

$$\mathfrak{u}_0^{\nu} = \gamma_1\mathfrak{u}_n^{\varepsilon} + \gamma_2\mathfrak{u}_m^{\delta} \in \operatorname{span}\big(\mathfrak{u}_n^{\varepsilon}, \mathfrak{u}_m^{\delta}\big) \subset \mathcal{K}. \tag{23}$$

A comparison of the coefficients at the same powers of ϵ yields up to first order in ϵ

$$\mathfrak{A}_{\alpha_0^{\nu}}\mathfrak{u}_0^{\nu} = \lambda_0^{\nu}\mathfrak{u}_0^{\nu}, \tag{24}$$

$$\mathfrak{A}_{\alpha_0^{\nu}}\mathfrak{u}_1 + \mathfrak{B}\mathfrak{u}_0^{\nu} = \lambda_0^{\nu}\mathfrak{u}_1 + \lambda_1\mathfrak{u}_0^{\nu}. \tag{25}$$

The first of these equations is satisfied identically, whereas the second one can be most conveniently analysed by projecting it with the help of the Krein space inner product $[.,.]$ onto the two-dimensional subspace[4] $\operatorname{span}\big(\mathfrak{u}_n^{\varepsilon}, \mathfrak{u}_m^{\delta}\big) \subset \mathcal{K}$

$$\big[\mathfrak{B}\mathfrak{u}_0^{\nu}, \mathfrak{u}_n^{\varepsilon}\big] = \lambda_1\big[\mathfrak{u}_0^{\nu}, \mathfrak{u}_n^{\varepsilon}\big], \qquad \big[\mathfrak{B}\mathfrak{u}_0^{\nu}, \mathfrak{u}_m^{\delta}\big] = \lambda_1\big[\mathfrak{u}_0^{\nu}, \mathfrak{u}_m^{\delta}\big]. \tag{26}$$

Using (23) in (26) yields a closed system of defining equations for the first-order spectral perturbation λ_1 and the coefficients γ_1 and γ_2:

$$\begin{pmatrix} \big[\mathfrak{B}\mathfrak{u}_n^{\varepsilon}, \mathfrak{u}_n^{\varepsilon}\big] - \lambda_1\big[\mathfrak{u}_n^{\varepsilon}, \mathfrak{u}_n^{\varepsilon}\big] & \big[\mathfrak{B}\mathfrak{u}_m^{\delta}, \mathfrak{u}_n^{\varepsilon}\big] \\ \big[\mathfrak{B}\mathfrak{u}_n^{\varepsilon}, \mathfrak{u}_m^{\delta}\big] & \big[\mathfrak{B}\mathfrak{u}_m^{\delta}, \mathfrak{u}_m^{\delta}\big] - \lambda_1\big[\mathfrak{u}_m^{\delta}, \mathfrak{u}_m^{\delta}\big] \end{pmatrix} \begin{pmatrix} \gamma_1 \\ \gamma_2 \end{pmatrix} = 0, \tag{27}$$

[4] The terms containing $\mathfrak{u}_1$ cancel due to the self-adjointness (6) of the operator $\mathfrak{A}_{\alpha_0^{\nu}}$ and equations (23) and (24).

i.e. in first-order approximation the perturbation $\epsilon\mathfrak{B}$ defines the spectral shift λ_1 and lifts the directional degeneration (23) of the zeroth-order eigenvectors $\mathfrak{u}_0^\nu$ by fixing two rays in the subspace $\mathrm{span}\big(\mathfrak{u}_n^\varepsilon, \mathfrak{u}_m^\delta\big) \subset \mathcal{K}$ (a standard effect also known from the perturbation theory of degenerate quantum mechanical systems [17]).

In our subsequent considerations of the system (27), we will need different explicit representations of the matrix elements containing $\mathfrak{B}$. Partial integration and substitution of the relation $\partial_r^2 u_n = [-\rho_n + l(l+1)/r^2]u_n$ give these representations as

$$\big[\mathfrak{B}\mathfrak{u}_m^\delta, \mathfrak{u}_n^\varepsilon\big] = \int_0^1 \varphi[(\rho_m + \varepsilon\delta\sqrt{\rho_n\rho_m})u_m u_n + u_m'' u_n + u_m' u_n']\,\mathrm{d}r \tag{28}$$

$$= \int_0^1 \varphi\left[\left(\varepsilon\delta\sqrt{\rho_n\rho_m} + \frac{l(l+1)}{r^2}\right) u_m u_n + u_m' u_n'\right]\mathrm{d}r. \tag{29}$$

The symmetry properties of equation (29) and its implication

$$\big[\mathfrak{B}\mathfrak{u}_m^\delta, \mathfrak{u}_n^\varepsilon\big] = \big[\mathfrak{B}\mathfrak{u}_n^\varepsilon, \mathfrak{u}_m^\delta\big] \tag{30}$$

are a natural consequence of the Krein space self-adjointness of the perturbation operator $\mathfrak{B}$ and the real valuedness of the eigenvectors $\mathfrak{u}_n^\varepsilon, \mathfrak{u}_m^\delta$.

From (27) and (30) we obtain the following defining equation for λ_1:

$$\lambda_1^2 - \lambda_1\left(\frac{\big[\mathfrak{B}\mathfrak{u}_n^\varepsilon, \mathfrak{u}_n^\varepsilon\big]}{\big[\mathfrak{u}_n^\varepsilon, \mathfrak{u}_n^\varepsilon\big]} + \frac{\big[\mathfrak{B}\mathfrak{u}_m^\delta, \mathfrak{u}_m^\delta\big]}{\big[\mathfrak{u}_m^\delta, \mathfrak{u}_m^\delta\big]}\right) + \frac{\big[\mathfrak{B}\mathfrak{u}_n^\varepsilon, \mathfrak{u}_n^\varepsilon\big]\big[\mathfrak{B}\mathfrak{u}_m^\delta, \mathfrak{u}_m^\delta\big] - \big[\mathfrak{B}\mathfrak{u}_n^\varepsilon, \mathfrak{u}_m^\delta\big]^2}{\big[\mathfrak{u}_n^\varepsilon, \mathfrak{u}_n^\varepsilon\big]\big[\mathfrak{u}_m^\delta, \mathfrak{u}_m^\delta\big]} = 0, \tag{31}$$

which with the Krein space norm (15) reduces to

$$\lambda_1^2 - \lambda_1\left(\varepsilon\frac{\big[\mathfrak{B}\mathfrak{u}_n^\varepsilon, \mathfrak{u}_n^\varepsilon\big]}{2\sqrt{\rho_n}} + \delta\frac{\big[\mathfrak{B}\mathfrak{u}_m^\delta, \mathfrak{u}_m^\delta\big]}{2\sqrt{\rho_m}}\right) + \varepsilon\delta\frac{\big[\mathfrak{B}\mathfrak{u}_n^\varepsilon, \mathfrak{u}_n^\varepsilon\big]\big[\mathfrak{B}\mathfrak{u}_m^\delta, \mathfrak{u}_m^\delta\big] - \big[\mathfrak{B}\mathfrak{u}_n^\varepsilon, \mathfrak{u}_m^\delta\big]^2}{4\sqrt{\rho_n\rho_m}} = 0. \tag{32}$$

This quadratic equation is of the type $\lambda_1^2 - \lambda_1(a_1 + a_2) + a_1a_2 - \varepsilon\delta b^2/4 = 0, a_1, a_2, b \in \mathbb{R}$, and its solutions $\lambda_{1,\pm} = [(a_1 + a_2) \pm \sqrt{(a_1 - a_2)^2 + \varepsilon\delta b^2}]/2$ are real valued for $\varepsilon = \delta$ and complex for $\varepsilon \neq \delta \cap (a_1 - a_2)^2 < b^2$ (in the present first-order approximation[5]). We see that they show the typical Krein space behaviour. Intersections of spectral branches corresponding to Krein space states of the same type ($\varepsilon = \delta$) induce no real-to-complex transitions in the spectrum (they are weak interactions in the sense of [18]). In contrast, intersections of spectral branches corresponding to states of different types ($\varepsilon \neq \delta$) may in general be accompanied by real-to-complex transitions (they are strong interactions in the sense of [18]). The same generic behaviour is implicitly present, e.g., in the $\mathcal{PT}$-symmetric quantum mechanical (QM) models of [19–23] (see also the discussion in [24, 25]). The unfolding of a diabolical point in a Hermitian QM model under $\mathcal{PT}$-symmetric perturbations was explicitly demonstrated in [26].

As noted above, the unfolding of the diabolical points is accompanied with a fixing of the directions of the zeroth-order eigenvectors $\mathfrak{u}_0^\nu \in \mathrm{span}\big(\mathfrak{u}_n^\varepsilon, \mathfrak{u}_m^\delta\big) \subset \mathcal{K}$. Using $\lambda_{1,\pm}$ in (27), one finds these directions as rays $\mathfrak{u}_{0,\pm}^\nu = \gamma_{1,\pm}\mathfrak{u}_n^\varepsilon + \gamma_{2,\pm}\mathfrak{u}_m^\delta$ defined by

$$\frac{\gamma_{1,\pm}}{\gamma_{2,\pm}} = -\frac{\big[\mathfrak{B}\mathfrak{u}_m^\delta, \mathfrak{u}_n^\varepsilon\big]}{\big[\mathfrak{B}\mathfrak{u}_n^\varepsilon, \mathfrak{u}_n^\varepsilon\big] - \big[\mathfrak{u}_n^\varepsilon, \mathfrak{u}_n^\varepsilon\big]\lambda_{1,\pm}} = -\frac{\big[\mathfrak{B}\mathfrak{u}_m^\delta, \mathfrak{u}_m^\delta\big] - \big[\mathfrak{u}_m^\delta, \mathfrak{u}_m^\delta\big]\lambda_{1,\pm}}{\big[\mathfrak{B}\mathfrak{u}_n^\varepsilon, \mathfrak{u}_m^\delta\big]}, \tag{33}$$

a generic result obtained, e.g., also in [16].

As part of the subsequent considerations, we will apply the general technique (28), (29), (32) and (33) for a detailed analytical study of the unfolding of diabolical points in concrete dynamo setups.

[5] Higher order corrections may lead to a further reduction of the real spectral sector.

4. Local deformations of the spectral mesh

The perturbation analysis of the previous section has been restricted to a first-order approximation—giving trustworthy analytical results for the behaviour of the spectrum in a close vicinity of any single diabolical point. Here we extend this approximation method to parameter space regions (α_0-regions) containing several diabolical points—allowing in this way to gain a qualitative understanding of how perturbations of the α-profile deform the spectral mesh over such a region. For this purpose, we extend the projection technique of the previous section from projecting on two-dimensional subspaces $\mathrm{span}\big(\mathfrak{u}_n^\varepsilon, \mathfrak{u}_m^\delta\big) \subset \mathcal{K}$ to projections on N-dimensional subspaces $\mathcal{L} := \mathrm{span}\big(\mathfrak{u}_{n_1}^{\varepsilon_1}, \ldots, \mathfrak{u}_{n_N}^{\varepsilon_N}\big) \subset \mathcal{K}$ spanned by those eigenvectors which are involved in the intersections over the concrete region. The method is well known from computational mathematics as the Galerkin method, the Rayleigh–Ritz method or the method of weighted residuals [27–31].

In order to simplify notations, we pass from double-indexed eigenvalues λ_n^ε and states $\mathfrak{u}_n^\varepsilon \in \mathcal{K}_\varepsilon \subset \mathcal{K}_+ \oplus \mathcal{K}_- \subset \mathcal{K}$ with $(n, \varepsilon) \in \mathbb{Z}^+ \times \mathbb{Z}_2 \sim \mathbb{Z}^* = \mathbb{Z} - \{0\}$ to eigenvalues[6] λ_n and normalized states $\mathfrak{v}_n$ depending only on the single state number[7] $n \in \mathbb{Z}^*$:

$$\lambda_n = \begin{cases} \lambda_n^+ & \text{for} \quad n \in \mathbb{Z}^+ \\ \lambda_{|n|}^- & \text{for} \quad n \in \mathbb{Z}^- \end{cases}, \qquad 2^{1/2}\rho_n^{1/4}\mathfrak{v}_n = \begin{cases} \mathfrak{u}_n^+ \in \mathcal{K}_+ & \text{for} \quad n \in \mathbb{Z}^+ \\ \mathfrak{u}_{|n|}^- \in \mathcal{K}_- & \text{for} \quad n \in \mathbb{Z}^- \end{cases} \tag{34}$$

with obvious implication

$$[\mathfrak{v}_n, \mathfrak{v}_m] = \varepsilon_n \delta_{nm}, \qquad \varepsilon_n := \mathrm{sign}(n). \tag{35}$$

Furthermore, we order the index set of the vectors of the subspace $\mathcal{L}$ according to the rule $n_1 > n_2 > \cdots > n_N$ with N_+ vectors $\mathfrak{v}_n$ of positive type and $N_- = N - N_+$ of negative type.

The approximation of the eigenvalue problem (1) consists in representing the eigenfunction $\mathfrak{u}$ as a linear combination

$$\mathfrak{u} = \sum_{k=1}^{N} c_k \mathfrak{v}_{n_k}, \qquad c_k \in \mathbb{C}, \tag{36}$$

over the finite set of basis functions $\{\mathfrak{v}_{n_k}\}_{k=1}^N$ and projecting[8] the resulting equation

$$\sum_{k=1}^{N} c_k \left(\mathfrak{A}_\alpha - \lambda\right) \mathfrak{v}_{n_k} = 0 \tag{37}$$

onto the subspace $\mathcal{L} = \mathrm{span}(\mathfrak{v}_{n_1}, \ldots, \mathfrak{v}_{n_N}) \subset \mathcal{K}$. In terms of the notation

$$\begin{aligned} &\tilde{\mathbf{A}}[\alpha] := (\tilde{A}_{ij})_{i,j=1}^N, \qquad \tilde{A}_{ij} := \left[\mathfrak{A}_\alpha \mathfrak{v}_{n_i}, \mathfrak{v}_{n_j}\right], \\ &\boldsymbol{\eta} := \mathrm{diag}\big(\varepsilon_{n_1}, \ldots, \varepsilon_{n_N}\big) = \begin{pmatrix} I_{N_+} & 0 \\ 0 & -I_{N_-} \end{pmatrix}, \\ &\mathbf{c} := (c_1, \ldots, c_N)^T \in \mathbb{C}^{N_+} \oplus \mathbb{C}^{N_-}, \end{aligned} \tag{38}$$

[6] We use the notation λ_n in spite of a possible ambiguity in the case of λ_1. From the concrete context, it will be clear whether the first-order perturbation λ_1 is considered or the spectral branch $\lambda_{n=1}$.

[7] Depending on the concrete context, we will subsequently use either double-indexed $\mathfrak{u}_n^\varepsilon$ or single-index $\mathfrak{v}_n$ notation for convenience.

[8] Given an exact solution $\mathfrak{u}_e$ of the eigenvalue problem $(\mathfrak{A}_\alpha - \lambda_e)\mathfrak{u}_e = 0$, the use of an approximate test function $\mathfrak{u} = \sum_{i=1}^N c_i \mathfrak{v}_{n_i}$ leads, in general, to a non-vanishing residual (error) $R(\mathbf{c}) := (\mathfrak{A}_\alpha - \lambda_e)\mathfrak{u}$, where $\mathbf{c} := (c_1, \ldots, c_N)^T$. The Galerkin method consists in solving the eigenvalue problem in a weak sense over the subspace $\mathcal{L}$ setting $[\mathfrak{v}_{n_i}, R(\mathbf{c})] = 0$ for each of the vectors $\mathfrak{v}_{n_i} \in \mathcal{L}$—fixing the initially undefined constants c_i. This implies that it yields exact solutions over the subspace $\mathcal{L}$ and a non-vanishing residual over the orthogonal complement $\mathcal{L}^{[\perp]} = \mathcal{K} \ominus \mathcal{L}$. The quality of the approximation can be naturally increased by increasing the dimension $N = \dim \mathcal{L}$. A relatively safe test for avoiding spurious solutions in numerical studies is to compare the output for approximations with different N. For details on the Galerkin method we refer to [30].

this leads to the simple $N \times N$-matrix eigenvalue problem

$$(\mathbf{A}[\alpha] - \lambda I_N)\mathbf{c} = 0, \qquad \mathbf{A}[\alpha] := \boldsymbol{\eta}^{-1}\tilde{\mathbf{A}}[\alpha] \tag{39}$$

with

$$\det(\mathbf{A}[\alpha] - \lambda I_N) = 0 \tag{40}$$

as defining equation for the spectral approximation[9]. A few comments are in order here.

First, we note that the reality of the eigenvectors $\mathfrak{v}_n$ and of the dynamo operator $\mathfrak{A}_\alpha$ (cf (2) and (14)) together with the self-adjointness of $\mathfrak{A}_\alpha$ in the Krein space $\mathcal{K}$ imply that the matrix $\tilde{\mathbf{A}}[\alpha]$ is real and symmetric, $\tilde{\mathbf{A}}^T[\alpha] = \tilde{\mathbf{A}}[\alpha]$. The Krein space related fundamental symmetry $\mathfrak{A}_\alpha = J\mathfrak{A}_\alpha^\dagger J$ (see (5)) is reflected in the structure of the matrix $\mathbf{A}[\alpha] = \boldsymbol{\eta}^{-1}\tilde{\mathbf{A}}[\alpha]$ as

$$\mathbf{A}[\alpha] = \boldsymbol{\eta}\mathbf{A}^T[\alpha]\boldsymbol{\eta}. \tag{41}$$

The involutory matrix $\boldsymbol{\eta} = \boldsymbol{\eta}^{-1}$ plays the role of a metric in the complex Pontryagin space[10] $\pi_\kappa = \mathbb{C}^{N_+} \oplus \mathbb{C}^{N_-} \ni \mathbf{c}$. In fact, it holds for $\mathfrak{u} = \sum_{i=1}^N c_i\mathfrak{v}_{n_i}$, $\mathfrak{w} = \sum_{j=1}^N d_j\mathfrak{v}_{n_j}$ that

$$[\mathfrak{u}, \mathfrak{w}] = \sum_{i,j=1}^N \bar{c}_i d_j [\mathfrak{v}_{n_i}, \mathfrak{v}_{n_j}] = \sum_{i=1}^N \varepsilon_{n_i}\bar{c}_i d_i = \bar{\mathbf{c}}^T\boldsymbol{\eta}\mathbf{d}. \tag{42}$$

Second, in the limit $N_\pm \to \infty$ the subspace $\mathcal{L}$ fills the whole Krein space $\mathcal{K}$ so that the approximation (36) of the vector $\mathfrak{u}$ tends to the exact representation $\mathfrak{u} = \sum_{n=-\infty}^\infty c_n\mathfrak{v}_n$ over the Krein space basis $\{\mathfrak{v}_n\}_{n=-\infty}^\infty$. In the same limit, the Pontryagin space π_κ tends to the Krein space $\mathcal{S} = \mathcal{S}_+ \oplus \mathcal{S}_- \ni \mathbf{c}$ with positive and negative type subspaces $\mathcal{S}_\pm$ as sequence spaces $\mathcal{S}_\pm = l_2(\mathbb{Z}^\pm)$. The determinant (40) becomes a Hill-type determinant. The mapping U from the eigenvalue problem (1) in the function space $\mathcal{K} \ni \mathfrak{u}$ to its equivalent representation (39) in the sequence space $\mathcal{S} \ni \mathbf{c}$

$$U : (\mathfrak{A}_\alpha - \lambda)\mathfrak{u} = 0 \quad \mapsto \quad (\mathbf{A}[\alpha] - \lambda)\mathbf{c} = 0 \tag{43}$$

is the Krein space equivalent of the well-known mapping from the quantum mechanical Schrödinger picture to its infinite-matrix representation in the Heisenberg picture [17]. In this sense, the described Galerkin method can be understood as an approximate solution technique based on a 'truncated Heisenberg representation' of the eigenvalue problem. Obviously, the method is not restricted to α^2-dynamo setups, rather in its present form it is applicable to any other Krein space related setup as well, like e.g. models of $\mathcal{PT}$-symmetric quantum mechanics. The only ingredient needed is a set of exactly known basis functions of an unperturbed operator.

In the next section, we use the described Galerkin method for a numerical analysis of the deformations of the spectral mesh in the region depicted in figure 1—leaving analytical estimates of the residual (the approximation error) to a forthcoming work[11].

[9] Representing $\alpha(r)$ as a function over a suitably chosen M-dimensional parameter space $\mathcal{M} \subseteq \mathbb{R}^M$, $\mathcal{M} \ni (p_1, \ldots, p_M, \alpha(r) = \alpha[r; p_1, \ldots, p_M]$, the determinant approximation (40) would allow for easy studies of the unfolding behaviour of the diabolical points over this parameter space. For example, for α-profiles $\alpha[r; p_1, \ldots, p_M] = \sum_{i=1}^M p_i f_i(r)$ with the parameters p_i as linear scale factors over a set of test functions $f_i(r)$, the determinant approximation (40) will lead to an algebraic equation $F(\lambda, p_1, \ldots, p_M) = 0$ of degree $\deg(F) = N$ in the spectral parameter λ and the parameters p_i. With the help of such an algebraic equation not only the unfolding of the diabolical points can be tested on their sensitivity with regard to changes of the function type $f_i(r)$, but rather the investigation of other (higher order) types of algebraic spectral singularities will be easily feasible. For a discussion (similar in spirit) on third-order branch points in $\mathcal{PT}$-symmetric matrix setups we refer to [25].

[10] A Krein space $\mathcal{K} = \mathcal{K}_+ \oplus \mathcal{K}_-$ is called a Pontryagin space π_κ when $\min(\dim\mathcal{K}_+, \dim\mathcal{K}_-) = \kappa < \infty$ [10].

[11] Collaborative work 'An operator model for the MHD α^2-dynamo' together with H Langer and C Tretter (in preparation).

5. The hyper-idealized s-wave ($l = 0$) sector and its α-resonance patterns

In this section, we consider the hyper-idealized case of zero spherical harmonics, $l = 0$, which in analogy to quantum scattering theory can be interpreted as an s-wave sector. Due to its too high symmetry contents, this sector does not play a role in the physics of spherical dynamos. There are no s-wave dynamos at all [2, 4]. Instead, it can be understood as a disc dynamo model [32]—in the concrete case of boundary conditions (4), as a disc dynamo with formal boundary conditions corresponding to a high-conductivity limit. Due to the strong spectral similarities of models with $l = 1$ and $l = 0$ (visible e.g. in figure 1), the study of disc dynamo models turns out very instructive from a technical point of view. Due to their highly simplified structure, they allow for a detailed analytical handling and a transparent demonstration of some of the essential mathematical features of the dynamo models. In our concrete context, they will provide some basic intuitive insight into the dynamo-related specifics of the unfolding of diabolical points. In the ($l \geqslant 1$)-sectors of the spherical models, these specifics will re-appear in a similar but more complicated way (see section 6).

Subsequently, we perform an analytical study of the local unfolding of the diabolical points (along the lines of section 3) that we supplement by numerical Galerkin results on the deformation of the spectral mesh.

Let $l = 0$. Then the differential expression of the operator $A_{l=0}$ simply reads $A_{l=0} = -\partial_r^2$ and $A_{l=0}$ has orthonormalized eigenfunctions $u_n(r)$, $u_n(0) = u_n(1) = 0$ and eigenvalues ρ_n

$$u_n = \sqrt{2}\sin(n\pi r), \qquad \rho_n = (\pi n)^2. \tag{44}$$

The eigenvalues of the matrix differential operator $\mathfrak{A}_{\alpha_0}$ are given as

$$\lambda_n^{\varepsilon} = -(\pi n)^2 + \varepsilon\alpha_0\pi n \tag{45}$$

and the corresponding eigenvectors $\mathfrak{u}_n^{\varepsilon}$ yield Krein space inner products

$$\left[\mathfrak{u}_n^{\varepsilon}, \mathfrak{u}_m^{\delta}\right] = \varepsilon 2\pi n\delta_{\varepsilon\delta}\delta_{mn} \tag{46}$$

and perturbation terms

$$\left[\mathfrak{B}\mathfrak{u}_m^{\delta}, \mathfrak{u}_n^{\varepsilon}\right] = 2\pi^2 mn\int_0^1 \varphi(r)\cos[(\delta m - \varepsilon n)\pi r]\,\mathrm{d}r. \tag{47}$$

According to (17), the diabolical points are located at points

$$\alpha_0^{\nu} = \pi(\varepsilon n + \delta m) =: \pi M, \qquad \lambda_0^{\nu} = \varepsilon\delta\pi^2 mn \tag{48}$$

and form a periodic vertical line structure in the (α_0, Re λ)-plane[12].

Inspection of the defining equation (31) for the first-order spectral perturbations λ_1 shows that this equation is invariant with regard to a rescaling of $\mathfrak{u}_n^{\varepsilon}$, $\mathfrak{u}_m^{\delta}$. Passing to the single-index notation (34) yields

$$\lambda_n = -(\pi n)^2 + \alpha_0\pi n, \qquad \mathfrak{v}_n(r) = \frac{1}{\sqrt{\pi|n|}}\begin{pmatrix}1\\ \pi n\end{pmatrix}\sin(\pi|n|r), \qquad n \in \mathbb{Z}^*, \tag{49}$$

with $[\mathfrak{v}_n, \mathfrak{v}_m] = \varepsilon_n\delta_{nm}$ and the following convenient representation of the perturbation terms (47):

$$[\mathfrak{B}\mathfrak{v}_{n+j}, \mathfrak{v}_n] = \pi\sqrt{|n(n+j)|}\int_0^1 \varphi(r)\cos(j\pi r)\,\mathrm{d}r. \tag{50}$$

[12] In the ($l \geqslant 1$)-sectors (for fixed $l \geqslant 1$), this line structure is approached asymptotically in the $|m|, |n| \to \infty$ limit. It follows from substituting the $l \ll |n| \to \infty$ limit of the Bessel function zeros [13] $\sqrt{\rho_{|n|}} \approx |n|\pi\,[1 + l/(2|n|)]$ into the expression for the α_0-coordinate (17) of the diabolical points: $\alpha_0^{\nu} = \varepsilon_n\sqrt{\rho_{|n|}} + \varepsilon_m\sqrt{\rho_{|m|}}$, $m, n \in \mathbb{Z}^*$.

This reduces the defining equation (32) for the spectral perturbation at the $(n, n+j)$ node of the spectral mesh (the intersection point of the λ_n and λ_{n+j} branches of the spectrum) with coordinates

$$\alpha_0^{\nu} = \pi(2n+j) =: \pi M, \qquad \lambda_0^{\nu} = \pi^2 n(n+j) \tag{51}$$

to

$$\lambda_1^2 - \lambda_1 \pi(2n+j) \int_0^1 \varphi(r)\,\mathrm{d}r + \pi^2 n(n+j) \times \left[\left(\int_0^1 \varphi(r)\,\mathrm{d}r \right)^2 - \left(\int_0^1 \varphi(r)\cos(j\pi r)\,\mathrm{d}r \right)^2 \right] = 0 \tag{52}$$

with solutions

$$\lambda_{1,\pm} = \frac{\pi}{2}(2n+j) \int_0^1 \varphi(r)\,\mathrm{d}r \pm \frac{\pi}{2} \sqrt{ j^2 \left(\int_0^1 \varphi(r)\,\mathrm{d}r \right)^2 + 4n(n+j) \left(\int_0^1 \varphi(r)\cos(j\pi r)\,\mathrm{d}r \right)^2 }. \tag{53}$$

We observe that the strength of the complex-valued unfolding of a diabolical point at a node with $n(n+j) < 0$ is defined by the relation between its $\cos(j\pi r)$-filtered perturbation $\int_0^1 \varphi(r)\cos(j\pi r)\,\mathrm{d}r$ and its average perturbation $\int_0^1 \varphi(r)\,\mathrm{d}r$.

A deeper insight into this peculiar feature of the unfolding process can be gained by expanding the perturbation φ in Fourier components over the interval [0, 1]

$$\varphi(r) = \frac{a_0}{2} + \sum_{k=1}^{\infty} [a_k \cos(2\pi k r) + b_k \sin(2\pi k r)] \tag{54}$$

with coefficients given as $a_0 = 2\int_0^1 \varphi(r)\,\mathrm{d}r$, $a_k = 2\int_0^1 \varphi(r)\cos(2\pi k r)\,\mathrm{d}r$, $b_k = 2\int_0^1 \varphi(r)\sin(2\pi k r)\,\mathrm{d}r$. In this way, the integral $\int_0^1 \varphi(r)\cos(j\pi r)\,\mathrm{d}r$ in (50) reduces to components of the type

$$\begin{aligned} &\int_0^1 \cos(j\pi r)\,\mathrm{d}r = \delta_{j,0}, \\ &\int_0^1 \cos(2\pi k r)\cos(j\pi r)\,\mathrm{d}r = \frac{1}{2}(\delta_{j,2k} + \delta_{-j,2k}), \\ &\int_0^1 \sin(2\pi k r)\cos(j\pi r)\,\mathrm{d}r = \begin{cases} 0 & \text{for} \quad j = \pm 2k \\ \dfrac{1-(-1)^j}{\pi} \dfrac{2k}{4k^2 - j^2} & \text{for} \quad j \neq \pm 2k \end{cases} \end{aligned} \tag{55}$$

and we obtain the perturbation terms (50) as

$$[\mathfrak{B}\mathfrak{v}_{n+j}, \mathfrak{v}_n] = \frac{\pi}{2}\sqrt{|n(n+j)|}\, Q_j, \tag{56}$$

$$Q_j := a_0 \delta_{j,0} + \sum_{k=1}^{\infty} \left[a_k(\delta_{j,2k} + \delta_{-j,2k}) + \frac{1-(-1)^j}{\pi} \frac{4b_k k}{4k^2 - j^2} \right]. \tag{57}$$

The defining quadratic equation for the spectral perturbation λ_1 now takes the form

$$\lambda_1^2 - \lambda_1 \frac{\pi}{2}(2n+j)a_0 + \frac{\pi^2}{4} n(n+j)\left(a_0^2 - Q_j^2\right) = 0 \tag{58}$$

and leads to the following very instructive representation for its solutions:

$$\lambda_{1,\pm} = \frac{\pi}{4}\big[(2n+j)a_0 \pm \sqrt{j^2 a_0^2 + 4n(n+j)\,Q_j^2}\big]. \tag{59}$$

The structure of these solutions shows that the unfolding of the diabolical points is controlled by several, partially competing, effects. Apart from the above-mentioned Krein space related feature of unfolding into real eigenvalues for states of the same Krein space type ($n(n+j) > 0$), and the possibility for unfolding into pairwise complex conjugate eigenvalues in the case of states of opposite type ($n(n+j) < 0$), a competition occurs between oscillating perturbations ($a_{k\neq 0}, b_k$) and homogeneous offset shifts a_0. In the case of vanishing offset shifts (mean perturbations), $a_0 = 0$, any inhomogeneous perturbation with $a_k, b_k \neq 0$ for some $k \geqslant 1$ leads for two branches with $n(n+j) < 0$ to a complex unfolding of the diabolical point. The strength of this complex directed unfolding becomes weaker when the homogeneous offset perturbation is switched on ($a_0 \neq 0$). There exists a critical offset

$$a_{0(c)}^2 := -\frac{4n(n+j)}{j^2}\,Q_j^2 \tag{60}$$

which separates the regions of real-valued and complex-valued unfoldings[13] (in the present first-order approximation). For $a_0^2 < a_{0(c)}^2 \cap n(n+j) < 0$ a complex-valued unfolding occurs, whereas for $a_0^2 > a_{0(c)}^2 \cap n(n+j) < 0$ the diabolical point unfolds real valued. The special case of a critical (balanced) perturbation $a_0^2 = a_{0(c)}^2 \cap n(n+j) < 0$ corresponds to an eigenvalue degeneration $\lambda_{1,+} = \lambda_{1,-} =: \lambda_{1(c)}$ which, because of (33), (34) and $\gamma_{1,+}\gamma_{2,+}^{-1} = \gamma_{1,-}\gamma_{2,-}^{-1}$, has coinciding zeroth-order rays so that via appropriate normalization the corresponding vectors $\mathfrak{v}_{0,+}^{\nu}, \mathfrak{v}_{0,-}^{\nu}$ can be made coinciding $\mathfrak{v}_{0,+}^{\nu} = \mathfrak{v}_{0,-}^{\nu} =: \mathfrak{v}_{0(c)}^{\nu}$. This means that the original diabolical point splits into a pair of exceptional (branch) points at perturbation configurations $a_0 = \pm|a_{0(c)}|$ with a Jordan chain consisting of the single (geometric) eigenvector (ray) $\mathfrak{v}_{0(c)}^{\nu}$ supplemented by an associated vector (algebraic eigenvector). This is in agreement with the unfolding scenario of diabolical points of general-type complex matrices described e.g. in [16].

Finally, the special case of $j = -2n$ is of interest. It corresponds to the intersection points located on the ($\alpha_0 = 0$)-axis of the (α_0, Re λ)-plane, where the operator matrix is self-adjoint not only in the Krein space $\mathcal{K}$, but also in the Hilbert space $\tilde{\mathcal{H}}$. Due to the vanishing factor $2n + j$, these diabolical points unfold via perturbations $\lambda_1 = \pm(\pi/2)|n|\sqrt{a_0^2 - a_{|n|}^2}$.

Let us now consider the strength of the unfolding contributions induced by certain Fourier components. For this purpose, we note that the diabolical points at nodes $(n, n+j)$ with the same absolute value of the index j are located on a parabolic curve[14]

$$\lambda_0^{\nu} = \frac{1}{4}\big(\alpha_0^{\nu 2} - \pi^2 j^2\big) = \frac{\pi^2}{4}(M^2 - j^2). \tag{61}$$

Due to its special role, we will refer to $j \in \mathbb{Z}$ as the parabola index ($M \in \mathbb{Z}$ is the index of the vertical line in the (α_0, Re λ)-plane defined in (48) and (51)). Furthermore, we see from the explicit structure of Q_j (following from expression (57))

$$Q_j = \begin{cases} \dfrac{8}{\pi}\displaystyle\sum_{k=1}^{\infty} b_k \frac{k}{4k^2 - j^2}, & j = \pm 1, \pm 3, \ldots \\ a_k(\delta_{j,2k} + \delta_{-j,2k}), & j = \pm 2, \pm 4, \ldots \end{cases} \tag{62}$$

[13] We note that for intersecting spectral branches it necessarily holds that $j \neq 0$, so that the offset term $a_0\delta_{j,0}$ in Q_j cancels and definition (60) of the critical offset $a_{0(c)}^2$ is justified.

[14] These (α_0, j)-parametrized parabolic curves coincide exactly with the spectral curves of a ($l = 0$)-sector model with physically realistic boundary conditions [36]. (For a discussion of physically realistic boundary conditions of spherically symmetric α^2-dynamos we refer to [2, 4].)

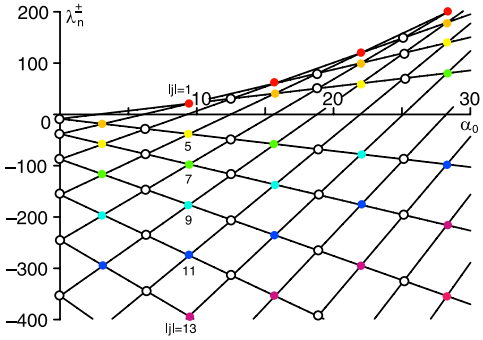

Figure 2. Odd harmonics of $\alpha(r)$ define the unfolding properties only of the coloured diabolical points (equally coloured DPs correspond to the same value of $|j|$), whereas even harmonics affect only the white (uncoloured) DPs.

that cosine and sine components of a similar order $|a_k| \sim |b_k|$ contribute differently at different nodes of the spectral mesh. It is remarkable that for all DPs with the same *even* $|j|$ (parabolas consisting of white points in figure 2), the splitting of the corresponding double eigenvalues depends (modulo the pre-factors $4n(n+j)$, j^2) only on the mean value a_0 of the perturbation $\varphi(r)$ and its $|j/2|$th cosine component $a_{|j/2|}$. For $n(n+j) < 0$ these contributions are competing, whereas for a strictly real-valued unfolding $n(n+j) > 0$ they enhance each other. Furthermore, we find from $M := 2n + j$ that the even/odd mode properties of j imply the same properties for M: even (odd) modes affect the unfolding of diabolical points at even (odd) M only. This is also clearly visible from figure 2.

In the more complicated case of *odd* parabola indices $|j|$, the splitting of the diabolical points on the parabola (61) (in figure 2 they are marked as points of the same colour) is governed by the competition between a_0 and the complete set of sine components b_k of the perturbation $\varphi(r)$. According to (62), a dominant role is played by sine harmonics with $j^2 \approx 4k^2$, i.e. with $k_\pm = (|j| \pm 1)/2$, such that a clear resonance and damping pattern occurs. Sine components with $j^2 \approx 4k^2$ are highly enhanced by a small denominator over the other sine components and the corresponding harmonics can be regarded as resonant ones. In contrast, sine contributions with modes away from the resonant $k_\pm = (|j| \pm 1)/2$ are strongly damped by the denominator $4k^2 - j^2$ and tend asymptotically to zero for $j^2 \to \infty$.

A first-order approximation based insight into this asymptotical behaviour can be gained from the positions of the exceptional points (EPs) in the $(\alpha_0, \mathrm{Re}\,\lambda)$-plane (the points where real-to-complex transitions occur). For this purpose, we use a 1D-lattice type parametrization for α_0 in form of $\alpha_0 = \alpha_0^\nu + \Delta\alpha_0 = \pi M + \Delta\alpha_0$, $M \in \mathbb{Z}$, and switch to a setting with $\epsilon = 1$ and $\Delta\alpha(r) := \varphi(r)$. Interpreting $\Delta\alpha_0$ as perturbation of a configuration with $\alpha_0^\nu = \pi M$ allows us to relate $\Delta\alpha_0$ to the Fourier coefficient $a_0 = 2\Delta\alpha_0$ and to estimate the α_0-positions of the EPs $\Delta\alpha_e(M, j)$ relative to their corresponding diabolical points located on the line $\alpha_0^\nu = \pi M$. Via (60) and $n = (M - j)/2$ we get for given Q_j

$$[\Delta\alpha_e(M, j)]^2 = -\frac{n(n+j)}{j^2} Q_j^2 = \frac{1}{4}\left(1 - \frac{M^2}{j^2}\right) Q_j^2. \tag{63}$$

For diabolical points in the lower $(\alpha_0, \mathrm{Re}\,\lambda)$-half-plane, it holds that $|j| \geqslant |M| + 2$ and (63) is well defined. In the case of cosine perturbations $a_k \cos(2\pi kr)$, (62) implies that only a single diabolical point per $M = 0, \pm 2, \pm 4, \ldots$ unfolds, whereas for sine perturbations $b_k \sin(2\pi kr)$ it leads to a countably infinite number of unfolding diabolical points per $M = \pm 1, \pm 3, \pm 5, \ldots$. Substituting (62) into (63) one obtains the $M^2, k^2 \ll j^2 \to \infty$ asymptotics of the EP

positions as

$$|\Delta\alpha_e(M, j)| \approx \frac{4|b_k|k}{\pi j^2}, \tag{64}$$

i.e. for increasing j^2 the distance of the EPs from the DPs is tending to zero. Conversely, (64) may be used to give an estimate for the number of complex eigenvalues for a given $\alpha_0 = \pi M + \Delta\alpha_0$ close[15] to a diabolical point line at $\alpha_0 \approx \pi M, |\Delta\alpha_0| \ll \pi : |j| \approx 2[k|b_k|/(\pi|\Delta\alpha_0|)]^{1/2}$.

Above, we arrived at the conclusion that both types of $|j|$-nodes (even ones and odd ones) show a similar collective behaviour along the parabolic curves (61) of fixed j^2, responding on some specific α-perturbation harmonics in a resonant way. Hence, a specific α-resonance pattern is imprinted in the spectral unfolding picture of the diabolical points. Let us now analyse these α-resonance patterns as imprints in the deformations of the spectral mesh. We study these deformations with the help of a Galerkin approximation over a 24-dimensional Krein subspace $\mathcal{L} = \mathrm{span}(\mathfrak{v}_{12}, \ldots, \mathfrak{v}_{-12}) \subset \mathcal{K}$—which is sufficient to cover the same spectral region as in figure 1. As α-profile we choose $\alpha(r) = \alpha_0 + \Delta\alpha(r)$ with pure harmonics $\Delta\alpha(r) = a_k \cos(2\pi kr)$ and $\Delta\alpha(r) = b_k \sin(2\pi kr)$, $k = 2, 3, 4$, $a_k = b_k = 5/2$, as perturbations[16]. The explicit structure of the corresponding Pontryagin space related matrix $\mathbf{A}[\alpha]$ (see (39)) is given in appendix B and yields the spectral approximations depicted in figure 3.

The most striking feature of the spectral deformations is their very clearly pronounced resonance character along parabolas with fixed index $|j|$—leaving spectral regions away from these resonance parabolas almost unaffected. Specifically, we find for *cosine* perturbations (depicted in the left column) that the harmonics $k = 2, 3, 4$ affect only the unfolding of diabolical points located strictly on the associated parabolas with index $j = 2k$. The effect of *sine* perturbations with mode numbers $k = 2, 3, 4$ is shown in the right column of figure 3. As predicted by (62), we find a strongly pronounced unfolding of diabolical points located on the parabolas with $|j| = 2k \pm 1$, that is for $|j| = 3$ and $|j| = 5$ (upper right picture), $|j| = 5$ and $|j| = 7$ (middle right picture) and $|j| = 7$ and $|j| = 9$ (lower right picture). The DPs with $|j| = 2k \pm m, m > 1$, are less affected and the strength of the unfolding quickly decreases with increasing distance m to the resonant parabolas. In addition to the unfolding effects predicted analytically by the first-order perturbation theory, the top and middle right pictures show additional DP unfoldings on the large-α_0 end of the $|j| = 2k$ parabola. The origin of these unfoldings can be attributed to higher order perturbative contributions.

The α-resonance pattern has a simple physical interpretation. Due to the fact that the spectral parameter implies an $e^{\lambda t}$ behaviour of the corresponding field mode, the α-resonance pattern shows that short scale perturbations of the α-profile (Fourier components with higher k) coherently affect faster decaying (more negative $\mathrm{Re}\,\lambda$) field modes than large scale perturbations with smaller k (which lead to smaller negative $\mathrm{Re}\,\lambda$).

Up to now we used the Galerkin method for investigations of weak perturbations over an $\alpha_0 = \mathrm{const}$ background. In figure 4, we demonstrate that the method works for strong perturbations as well. We observe that, increasing the strength of the pure harmonic perturbations from $a_2, b_2 = 5$ up to $a_2, b_2 = 30$, the regions with complex conjugate spectral contributions grow and finally intersect each other. Additionally, they shift into the upper $(\alpha_0, \mathrm{Re}\,\lambda)$-plane leading to overcritical oscillatory dynamo regimes ($\mathrm{Re}\,\lambda > 0, \mathrm{Im}\,\lambda \neq 0$).

[15] The first-order approximation (63) leads to a third-order polynomial $F(\Delta\alpha_e, j^2) = 0$ in j^2. Its solutions are of limited meaning because of possible contributions from higher order perturbation terms.

[16] The amplitudes a_k, b_k have been chosen as large as $a_k = b_k = 5/2 > 1$ in order to clearly demonstrate the unfolding pattern.

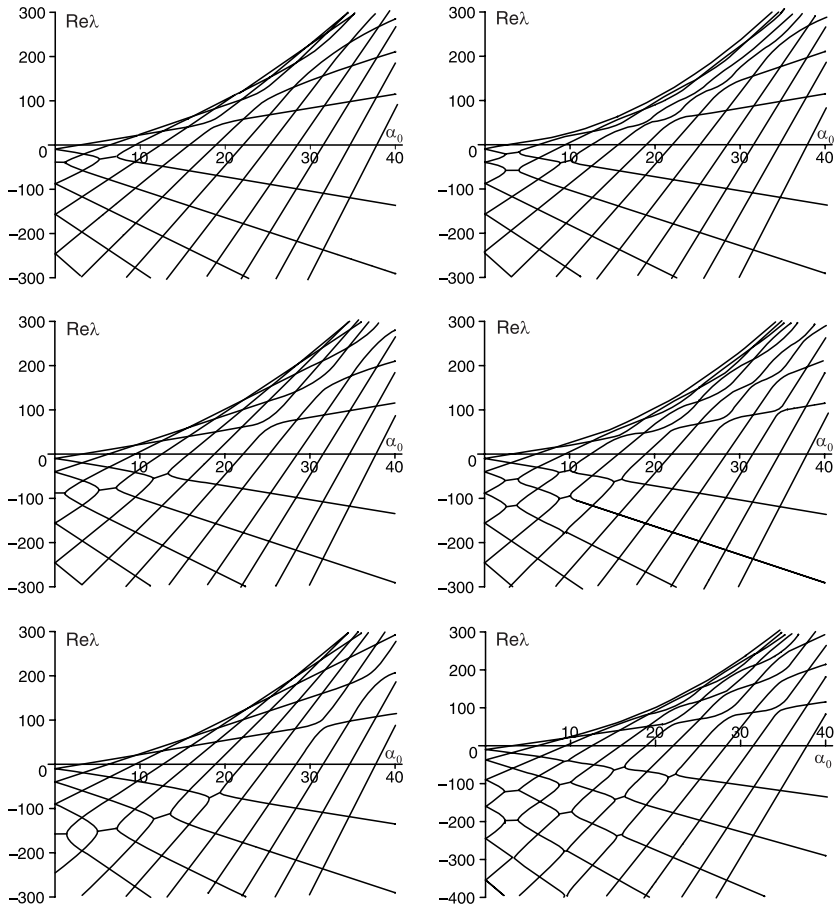

Figure 3. Resonant deformation of the spectral mesh with resonant unfolding of diabolical points due to perturbations by pure harmonics. Left column (top to bottom): $\Delta\alpha(r) = 2.5\cos(4\pi r)$, $\Delta\alpha(r) = 2.5\cos(6\pi r)$, $\Delta\alpha(r) = 2.5\cos(8\pi r)$; right column (top to bottom): $\Delta\alpha(r) = 2.5\sin(4\pi r)$, $\Delta\alpha(r) = 2.5\sin(6\pi r)$, $\Delta\alpha(r) = 2.5\sin(8\pi r)$.

An estimate of critical α-profiles, for which such a transition to the upper $(\alpha_0, \mathrm{Re}\,\lambda)$-half-plane starts to occur, can be given within a first-order (linear) perturbative approximation by assuming $\mathrm{Re}\,\lambda(\alpha_0) = 0$ for the exceptional point closest to the $(\mathrm{Re}\,\lambda = 0)$-line. Relations (61), (63) and $\mathrm{Re}\,\lambda = \lambda_0^\nu + \mathrm{Re}\,\lambda_1 = \lambda_0^\nu + \pi M a_0/4$ yield this condition in terms of the Fourier components Q_j of such a critical α-profile as

$$\mathrm{Re}\,\lambda = \frac{\pi^2}{4}(M^2 - j^2) + \frac{\pi}{4}M\left(1 - \frac{M^2}{j^2}\right)^{1/2}|Q_j| = 0. \tag{65}$$

This relation may be used for testing concrete α-profiles on their capability to produce complex eigenvalues in the right spectral half-plane $(\mathrm{Re}\,\lambda > 0, \mathrm{Im}\,\lambda \neq 0)$.

We restrict our present consideration of $(l = 0)$-models to this first numerical output and the analytical estimate, expecting physically more relevant results from extending the present methods to models with physically realistic boundary conditions. In the next section, we present some first few results on the $(l \geqslant 1)$-sectors of the α^2-dynamo model.

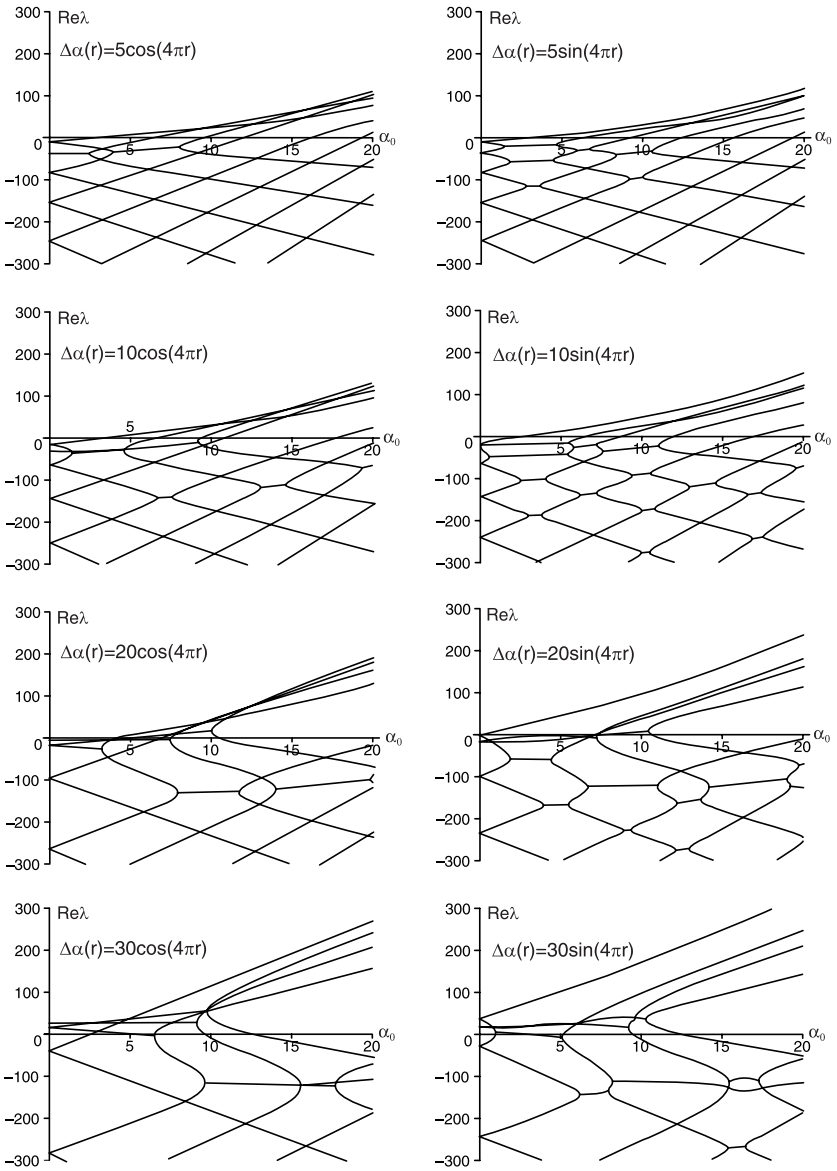

Figure 4. Resonant deformation of the spectral mesh under strong and ultra-strong perturbations of pure harmonic type: $\Delta\alpha(r) = a_2 \cos(4\pi r)$ (left column) and $\Delta\alpha(r) = b_2 \sin(4\pi r)$ (right column) with $a_2, b_2 = 5, 10, 20, 30$. Strong perturbations lead not only to large spectral regions with complex conjugate eigenvalues, but also to a lifting of the corresponding complex branches into the upper $(\alpha_0, \mathrm{Re}\,\lambda)$-plane, i.e. they lead to overcritical dynamo regimes ($\mathrm{Re}\,\lambda > 0$) of oscillatory type ($\mathrm{Im}\,\lambda \neq 0$).

6. Numerical techniques and examples for the ($l \geqslant 1$)-sectors

In this section, we reshape the general results of section 3 in a form suitable for numerical investigations and demonstrate them on a first concrete model from the ($l = 1$)-sector.

We start by representing the perturbation terms $\left[\mathfrak{B}\mathfrak{u}_m^\delta, \mathfrak{u}_n^\varepsilon\right]$ from equations (28) and (29) as

$$\begin{aligned}\left[\mathfrak{B}\mathfrak{u}_m^\delta, \mathfrak{u}_n^\varepsilon\right] &= \int_0^1 \varphi\left[\left(\varepsilon\delta\sqrt{\rho_m\rho_n} + \frac{l(l+1)}{r^2}\right)u_m u_n + u_m' u_n'\right]\mathrm{d}r \\ &= 2(\rho_m\rho_n)^{1/4}\int_0^1 \varphi(r) g_{mn}^l(r)\,\mathrm{d}r, \qquad m,n\in\mathbb{Z}^+,\end{aligned} \tag{66}$$

or equivalently

$$\begin{aligned}[\mathfrak{B}\mathfrak{v}_m, \mathfrak{v}_n] &= \int_0^1 \varphi\left[\left(\varepsilon_m\varepsilon_n\sqrt{\rho_{|m|}\rho_{|n|}} + \frac{l(l+1)}{r^2}\right)u_{|m|}u_{|n|} + u_{|m|}' u_{|n|}'\right]\mathrm{d}r \\ &= \int_0^1 \varphi(r) g_{mn}^l(r)\,\mathrm{d}r, \qquad m,n\in\mathbb{Z}^*.\end{aligned} \tag{67}$$

The functions g_{mn}^l are symmetric $g_{mn}^l = g_{nm}^l$ and from the Fréchet (functional) derivative[17]

$$\frac{\delta[\mathfrak{B}\mathfrak{v}_m, \mathfrak{v}_n]}{\delta\varphi(r)} \equiv \nabla_\varphi[\mathfrak{B}\mathfrak{v}_m, \mathfrak{v}_n] = g_{mn}^l(r) \tag{68}$$

we find that they can be naturally interpreted as components of the perturbation gradient in the Krein space $\mathcal{K}$. Their explicit representation in terms of Bessel functions is given in appendix C. Representation (66) may prove especially useful for the optimization of α-profiles with regard to given constraints or experimental requirements.

First, we note that in terms of the gradient functions $g_{mn}^l(r)$ the defining equation (32) for the first-order spectral perturbations λ_1 reduces to

$$\begin{aligned}&\lambda_1^2 - \lambda_1\int_0^1 \varphi\left(\varepsilon g_{nn}^l + \delta g_{mm}^l\right)\mathrm{d}r \\ &\qquad + \varepsilon\delta\left[\left(\int_0^1 \varphi g_{mm}^l\,\mathrm{d}r\right)\left(\int_0^1 \varphi g_{nn}^l\,\mathrm{d}r\right) - \left(\int_0^1 \varphi g_{mn}^l\,\mathrm{d}r\right)^2\right] = 0\end{aligned} \tag{69}$$

with solutions

$$\lambda_{1,\pm} = \frac{1}{2}\int_0^1 \varphi\left(\varepsilon g_{nn}^l + \delta g_{mm}^l\right)\mathrm{d}r \pm \frac{1}{2}\sqrt{\left[\int_0^1 \varphi\left(\varepsilon g_{nn}^l - \delta g_{mm}^l\right)\mathrm{d}r\right]^2 + 4\varepsilon\delta\left[\int_0^1 \varphi g_{mn}^l\,\mathrm{d}r\right]^2}. \tag{70}$$

Comparison with the results for the hyper-idealized s-wave sector (disc dynamo) shows that apart from the generic Krein space related behaviour (no complex eigenvalues for intersecting spectral branches of the same type, $\delta = \varepsilon$, and possible formation of complex eigenvalues for branches of different type, $\varepsilon \neq \delta$) we find a generalization of the offset and oscillation contributions for $\varepsilon \neq \delta$ type intersections. In rough analogy, the role of a transition preventing offset is played by the 'diagonal' terms

$$\int_0^1 \varphi\left(g_{nn}^l + g_{mm}^l\right)\mathrm{d}r \tag{71}$$

whereas the 'off-diagonal' terms

$$\int_0^1 \varphi g_{mn}^l\,\mathrm{d}r \tag{72}$$

[17] The Fréchet derivative $\nabla f(x)$ of a function $f(x)$ over an open set $X \ni x$ of a Banach space $F \supset X$ is defined as $f(x+u) - f(x) = \nabla f(x)u + o(\|u\|)$ [33–35] which for the functional $f(\varphi) := [\mathfrak{B}\mathfrak{v}_m, \mathfrak{v}_n]$ can be reshaped as $f(\varphi+\chi) - f(\varphi) = (\nabla_\varphi f(\varphi), \chi) + o(\|\chi\|)$.

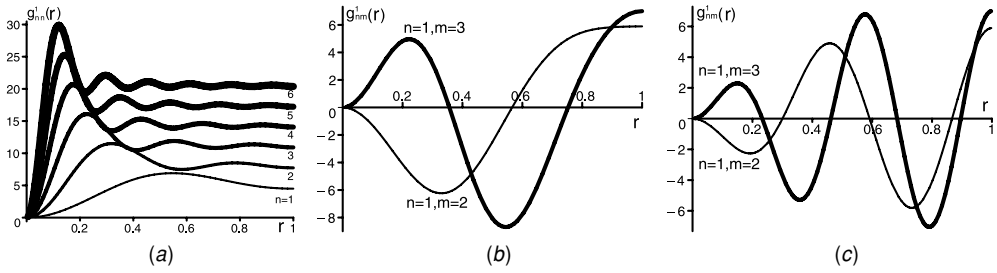

Figure 5. Functions $g^l_{nm}(r)$ for $l = 1$, $n = m$ (a) and $n = 1$, $m = 2, 3$ in the cases $\varepsilon\delta = 1$ (b) and $\varepsilon\delta = -1$ (c).

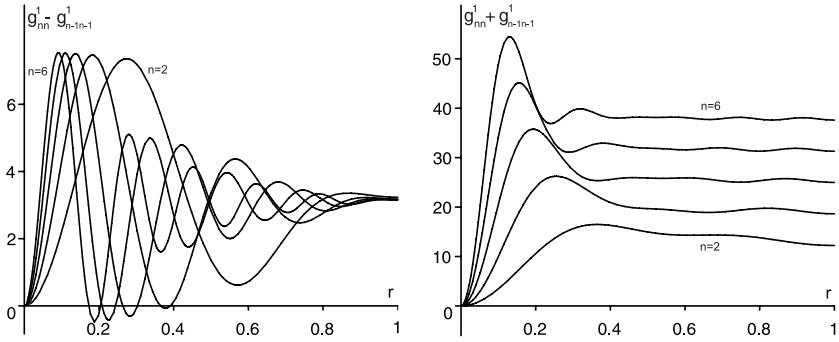

Figure 6. Gradient function differences $g^1_{nn}(r) - g^1_{n-1n-1}(r)$ as they enhance the real-valued unfolding of diabolical points in the upper $(\alpha_0, \mathrm{Re}\,\lambda)$-plane (left), as well as offset gradient functions (integration kernels) of the type $g^1_{nn}(r) + g^1_{n-1n-1}(r)$ for $n = 2, \ldots, 6$ (right).

enhance a possible transitions to complex eigenvalues, i.e. a transition occurs for

$$\varepsilon \neq \delta \cap \left(\frac{1}{2}\int_0^1 \left(g^l_{nn} + g^l_{mm}\right)\varphi \,\mathrm{d}r\right)^2 < \left(\int_0^1 g^l_{mn}\varphi \,\mathrm{d}r\right)^2. \tag{73}$$

Condition (73) yields an explicit classification criterion for α-profile perturbations with regard to their capability to induce complex eigenvalues. It may serve as an efficient search tool for concrete $\alpha(r)$-profiles—and transforms in this way some general observations of [4] into a technique of direct applicability.

The functions $g^l_{nm}(r)$ for $l = 1$ and different values of n, m and $\varepsilon\delta$ are shown in figure 5. One clearly sees that the 'diagonal' functions with $m = n$ are always non-negative and the graphics of any two of them, $g^1_{nn}(r)$, $g^1_{mm}(r)$ with $m \neq n$, intersect only marginally (see figure 6). Their sums $g^1_{nn}(r) + g^1_{mm}(r)$ are strictly sign-preserving functions so that they act as an averaging integration kernel. In contrast, the 'off-diagonal' functions $g^1_{nm}(r)$ with $m \neq n$ show strong sign changes and in this way they act as a filter kernel. Hence, the main qualitative roles of the 'diagonal' and 'off-diagonal' functions as 'offset' and 'oscillation filter' functions remain preserved also for the $(l = 1)$-sector. Their subtle interplay is crucial for the α-profile to act as generator of complex eigenvalues.

As in the $(l = 0)$-sector, spectral deformations over a certain parameter space region can be studied numerically. For α-profiles $\alpha(r) = \alpha_0 + \Delta\alpha(r)$, the corresponding approximation

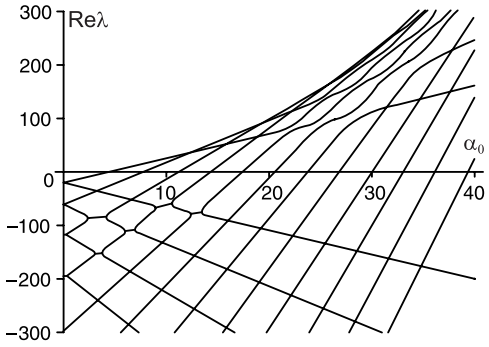

Figure 7. Deformations of the spectral mesh with unfolding of diabolical points for the $(l = 1)$-sector of a model with $\alpha(r) = \alpha_0 + 2.5\cos(6\pi r)$.

matrix of the Galerkin method simply reads

$$A_{mn}[\alpha] = \lambda_m \delta_{mn} + \varepsilon_m \int_0^1 \Delta\alpha(r) g^l_{mn}(r)\,\mathrm{d}r. \tag{74}$$

In figure 7, we illustrate the method for an α-profile $\alpha(r) = \alpha_0 + 2.5\cos(6\pi r)$ and a similar approximation subspace $\mathcal{L} = \mathrm{span}(\mathfrak{v}_{12}, \ldots, \mathfrak{v}_{-12}) \subset \mathcal{K}$ as in the previous section. For the $(l = 1)$-mode Riccati–Bessel functions, a cosine perturbation is no longer an exact resonance mode and the deformations of the mesh spread over a broader parabola-like region.

Finally, we note that explicit analytical considerations of the spectrum in the $(l > 0)$-sector are obstructed by the lack of simple transformation rules between Riccati–Bessel functions as well as of simple expressions for integrals over triple products of spherical Bessel functions in the case of finite integration intervals.

7. Conclusions and discussions

In the present work, the spectral properties of spherically symmetric MHD α^2-dynamos with idealized boundary conditions have been studied. Using the fundamental symmetry of the dynamo operator matrix and the solution set of a model with constant α-profile, a Krein space related perturbation theory as well as a Galerkin technique for numerical investigations has been developed. As an analytical result of the first-order perturbation theory, we found a strongly pronounced α-resonance pattern in the unfolding of diabolical points. The resonance behaviour reflects the correspondence between the characteristic length scale of α-perturbations and the decay rates of the coherently induced field excitations. The observed correlations will strongly affect the specifics of reversal processes of dynamo maintained magnetic fields [37, 38] and support corresponding numerical simulations on more realistic dynamo setups [39]. An estimation technique has been developed for obtaining the critical α-profiles at which the eigenvalues enter the right spectral half-plane with non-vanishing imaginary components (at which overcritical oscillatory dynamo regimes form). This technique has been demonstrated explicitly for the $(l = 0)$-sector, where it leads to a bound on the Fourier components of the α-profile. The analytical results on the perturbative unfolding of diabolical points have been supplemented by numerical studies of the deformations of the dynamo operator spectrum. The capability of the used Galerkin approach has been demonstrated in extending the strength of the α-perturbations from weakly perturbed regimes up to ultra-strong perturbations. Extensions of the presented techniques to

spherically symmetric α^2-dynamos with realistic boundary conditions as well as to models of $\mathcal{PT}$-symmetric quantum mechanics are straightforward.

Acknowledgments

We thank G Gerbeth, H Langer and C Tretter for useful discussions, and F Stefani and M Xu additionally for cross-checking our Galerkin-based results with other numerical codes. This work has been supported by the German Research Foundation DFG, grant GE 682/12-2 (UG), as well as by the CRDF-BRHE program and the Alexander von Humboldt Foundation (ONK).

Appendix A. Bessel function relations

The solutions $u_n(r)$ of the eigenvalue problem (9)

$$A_l u_n = \rho_n u_n, \qquad u_n(r\searrow 0) = u_n(r=1) = 0, \qquad A_l = -\partial_r^2 + \frac{l(l+1)}{r^2} \tag{A.1}$$

are so-called Riccati–Bessel functions [13]

$$u_n(r) \sim \sqrt{\rho_n} r j_l(\sqrt{\rho_n} r), \tag{A.2}$$

where $j_l(\sqrt{\rho_n} r)$ denote spherical Bessel functions. They can be expressed in terms of Bessel functions $J_{l+\frac{1}{2}}(\sqrt{\rho_n} r)$ and for definiteness we represent the solutions u_n as

$$u_n(r) = N_n \sqrt{r} J_{l+\frac{1}{2}}(\sqrt{\rho_n} r) \tag{A.3}$$

with N_n a normalization coefficient.

The orthogonality of these solutions can be easily verified with the help of well-known Bessel function relations [13, 40, 41]. For $m \neq n$, it holds that

$$\begin{aligned}(u_m, u_n) &= N_m N_n \int_0^1 r J_{l+\frac{1}{2}}(\sqrt{\rho_m} r) J_{l+\frac{1}{2}}(\sqrt{\rho_n} r)\,\mathrm{d}r \\ &= N_m N_n \frac{r}{\rho_m - \rho_n}\left[J_{l+\frac{1}{2}}(\sqrt{\rho_m} r)\partial_r J_{l+\frac{1}{2}}(\sqrt{\rho_n} r) - J_{l+\frac{1}{2}}(\sqrt{\rho_n} r)\partial_r J_{l+\frac{1}{2}}(\sqrt{\rho_m} r)\right]\Big|_0^1.\end{aligned} \tag{A.4}$$

This expression vanishes because of $J_{l+\frac{1}{2}}(0) = J_{l+\frac{1}{2}}(\sqrt{\rho_n}) = 0$ and $|\partial_r J_{l+\frac{1}{2}}(\sqrt{\rho_k} r)|_{r\searrow 0} < \infty$. In a similar way, it holds that [13, 40, 41]

$$\begin{aligned}\|u_n\|^2 = (u_n, u_n) &= N_n^2 \int_0^1 r J_{l+\frac{1}{2}}^2(\sqrt{\rho_n} r)\,\mathrm{d}r = \frac{1}{2} N_n^2 \left[\partial_r J_{l+\frac{1}{2}}(\sqrt{\rho_n} r)\right]^2\Big|_{r=1} \\ &= \frac{1}{2} N_n^2 J_{l+\frac{3}{2}}^2(\sqrt{\rho_n}),\end{aligned} \tag{A.5}$$

so that $N_n = \sqrt{2}/J_{l+\frac{3}{2}}(\sqrt{\rho_n})$ gives $(u_n, u_n) = 1$.

Appendix B. Explicit structure of the approximation matrix $\mathbf{A}[\alpha]$

In the $(l = 0)$-sector, the relations (49), (50) and (56) lead for the approximation matrix $\mathbf{A}[\alpha] = \boldsymbol{\eta}^{-1}(\tilde{A}_{mn})_{m,n=-N}^{N}$, $\tilde{A}_{mn} = [\mathfrak{A}_\alpha \mathfrak{v}_m, \mathfrak{v}_n]$, of (39) over an α-profile $\alpha(r) = \alpha_0 + \Delta\alpha(r)$ to the following structure:

$$\begin{aligned}A_{mn}[\alpha] &= \lambda_m \delta_{mn} + \varepsilon_m \pi \sqrt{|mn|} \int_0^1 \Delta\alpha(r) \cos[(m-n)\pi r]\,\mathrm{d}r \\ &= [-(\pi m)^2 + \alpha_0 \pi m]\delta_{mn} + \varepsilon_m \frac{\pi}{2}\sqrt{|mn|}\, Q_{m-n}.\end{aligned} \tag{B.1}$$

In the case of $\Delta\alpha(r) = a_k \cos(2\pi kr)$, this gives

$$A_{mn}[\alpha_0, a_k] = [-(\pi m)^2 + \alpha_0 \pi m]\delta_{mn} + \varepsilon_m \frac{\pi}{2}\sqrt{|mn|}a_k(\delta_{m,n+2k} + \delta_{m,n-2k}), \tag{B.2}$$

i.e. $\mathbf{A}[\alpha]$ has the eigenvalues λ_m of the unperturbed $\mathfrak{A}_{\alpha_0}$ on its diagonal and possesses two subdiagonals with non-vanishing entries a distance $\pm 2k$ aside the main diagonal. For perturbations $\Delta\alpha(r) = b_k \sin(2\pi kr)$, one finds

$$A_{mn}[\alpha_0, b_k] = [-(\pi m)^2 + \alpha_0 \pi m]\delta_{mn} + \varepsilon_m \sqrt{|mn|}[1 - (-1)^{m-n}]\frac{2kb_k}{4k^2 - (m-n)^2}. \tag{B.3}$$

Appendix C. Explicit expressions for the gradient functions $g^l_{mn}(r)$

Explicit expressions for the gradient components $g^l_{mn}(r)$ can be derived from the representation (10) of the eigenfunctions $u_n^{\varepsilon_n}$ and the defining relation (66). As a result, one obtains in $(n, \varepsilon_n) \in \mathbb{Z}^+ \times \mathbb{Z}_2$ notations

$$\begin{aligned} g^l_{mn}(r) = {} & \frac{(\varepsilon_m\varepsilon_n\sqrt{\rho_m\rho_n}r^2 + l^2 + l)J_{l+1/2}(r\sqrt{\rho_m})J_{l+1/2}(r\sqrt{\rho_n})}{r(\rho_m\rho_n)^{1/4}J_{l-1/2}(\sqrt{\rho_m})J_{l-1/2}(\sqrt{\rho_n})} \\ & + \frac{[r\sqrt{\rho_m}J_{l-1/2}(r\sqrt{\rho_m}) - lJ_{l+1/2}(r\sqrt{\rho_m})][r\sqrt{\rho_n}J_{l-1/2}(r\sqrt{\rho_n}) - lJ_{l+1/2}(r\sqrt{\rho_n})]}{r(\rho_m\rho_n)^{1/4}J_{l-1/2}(\sqrt{\rho_m})J_{l-1/2}(\sqrt{\rho_n})} \end{aligned} \tag{C.1}$$

and $g^l_{mn}(r = 1) = (\rho_m\rho_n)^{1/4}$.

References

[1] Moffatt H K 1978 *Magnetic Field Generation in Electrically Conducting Fluids* (Cambridge: Cambridge University Press)

[2] Krause F and Rädler K-H 1980 *Mean-Field Magnetohydrodynamics and Dynamo Theory* (Berlin/Oxford: Academic/Pergamon) chapter 14

[3] Zeldovich Ya B, Ruzmaikin A A and Sokoloff D D 1983 *Magnetic Fields in Astrophysics* (New York: Gordon and Breach)

[4] Günther U and Stefani F 2003 *J. Math. Phys.* **44** 3097 (*Preprint* math-ph/0208012)

[5] Günther U, Stefani F and Znojil M 2005 *J. Math. Phys.* **46** 063504 (*Preprint* math-ph/0501069)

[6] Proctor M R E 1977 *Astron. Nachr.* **298** 19
Proctor M R E 1977 *Geophys. Astrophys. Fluid Dyn.* **8** 311
Rädler K-H 1982 *Geophys. Astrophys. Fluid Dyn.* **20** 191
Rädler K-H and Geppert U 1999 Turbulent dynamo action in the high-conductivity limit: a hidden dynamo *Workshop on Stellar Dynamos (ASP Conf. Ser. 178)* ed M Nunez and A Ferriz-Mas p 151

[7] Bognár J 1974 *Indefinite Inner Product Spaces* (New York: Springer)

[8] Langer H 1982 *Functional Analysis (Lecture Notes in Mathematics* vol 948*)* (Berlin: Springer) p 1

[9] Azizov T Ya and Iokhvidov I S 1989 *Linear Operators in Spaces With an Indefinite Metric* (New York: Wiley–Interscience)

[10] Dijksma A and Langer H 1996 Operator theory and ordinary differential operators *Lectures on Operator Theory and its Applications (Fields Institute Monographs* vol 3*)* ed A Böttcher *et al* (Providence, RI: American Mathematical Society) p 75

[11] Langer H and Tretter C 2004 *Czech. J. Phys.* **54** 1113–20

[12] Berry M V and Wilkinson M 1984 *Proc. R. Soc.* A **392** 15

[13] Abramowitz M and Stegun I A 1964 *Handbook of Mathematical Functions* (Washington, DC: National Bureau of Standards)

[14] Kato T 1966 *Perturbation Theory for Linear Operators* (Berlin: Springer)

[15] Baumgärtel H 1984 *Analytic Perturbation Theory for Matrices and Operators* (Berlin: Academic)
Baumgärtel H 1985 *Analytic Perturbation Theory for Matrices and Operators (Operator Theory: Advances and Applications* vol 15*)* (Basle: Birkhauser)

[16] Kirillov O N, Mailybaev A A and Seyranian A P 2005 *J. Phys. A: Math. Gen.* **38** 5531–46 (*Preprint* math-ph/0411006)
[17] Landau L D and Lifshitz E M 1965 *Quantum Mechanics: Non-Relativistic Theory* (Oxford: Pergamon)
[18] Seyranian A P, Kirillov O N and Mailybaev A A 2005 *J. Phys. A: Math. Gen.* **38** 1723–40 (*Preprint* math-ph/0411024)
[19] Znojil M 2001 What is PT symmetry? *Preprint* quant-ph/0103054 version 1
Znojil M 2004 *Rendic. Circ. Mat. Palermo, Ser. II, Suppl.* **72** 211–8 (*Preprint* math-ph/0104012)
[20] Dorey P, Dunning C and Tateo R 2001 *J. Phys. A: Math. Gen.* **34** L391 (*Preprint* hep-th/0104119)
[21] Mostafazadeh A 2002 *J. Math. Phys.* **43** 6343–52 (*Preprint* math-ph/0207009)
Mostafazadeh A 2003 *J. Phys. A: Math. Gen.* **36** 7081–92 (*Preprint* quant-ph/0304080)
[22] Bender C M, Brody D C and Jones H F 2002 *Phys. Rev. Lett.* **89** 270401 (*Preprint* quant-ph/0208076)
Bender C M, Brody D C and Jones H F 2003 *Am. J. Phys.* **71** 1095–102 (*Preprint* hep-th/0303005)
[23] Bender C M, Meisinger P N and Wang Q 2003 *J. Phys. A: Math. Gen.* **36** 6791 (*Preprint* quant-ph/0303174)
[24] Günther U, Stefani F and Gerbeth G 2004 *Czech. J. Phys.* **54** 1075–90 (*Preprint* math-ph/0407015)
[25] Günther U and Stefani F 2005 *Czech. J. Phys.* **55** 1099–106 (*Preprint* math-ph/0506021)
[26] Caliceti E, Graffi S and Sjöstrand J 2005 *J. Phys. A: Math. Gen.* **38** 185–93 (*Preprint* math-ph/0407052)
[27] Gottlieb D and Orszag S A 1977 *Numerical Analysis of Spectral Methods: Theory and Applications* (Philadelphia, PA: SIAM)
[28] Bender C M and Orszag S A 1999 *Advanced Mathematical Methods for Scientists and Engineers* (New York: Springer)
[29] Fletcher C A J 1984 *Computational Galerkin Methods* (New York: Springer)
[30] Boyd J P 2001 *Chebyshev and Fourier Spectral Methods* (New York: Dover)
[31] Atkinson K and Han W 2005 *Theoretical Numerical Analysis: A Functional Analysis Framework* (New York: Springer)
[32] Baryshnikova Y and Shukurov A 1987 *Astron. Nachr.* **308** 89–100
[33] Kadets M I and Kadets V M 1997 *Series in Banach Spaces (Operator Theory: Advances and Applications* vol 94*)* (Basle: Birkhauser)
[34] Benyamini Y and Lindenstrauss J 2000 *Geometric Nonlinear Functional Analysis* vol 1 (Providence, RI: American Mathematical Society)
[35] Abramovich Y A and Aliprantis C D 2002 *An Invitation to Operator Theory* (Providence, RI: American Mathematical Society)
[36] Günther U and Kirillov O Asymptotic techniques for spherically symmetric MHD α^2-dynamos (in preparation)
[37] Stefani F and Gerbeth G 2005 *Phys. Rev. Lett.* **94** 184506 (*Preprint* physics/0411050)
[38] Stefani F, Gerbeth G, Günther U and Xu M 2006 Why dynamos are prone to reversals *Earth Planet. Sci. Lett.* **243** 828–40 (*Preprint* physics/0509118)
[39] Giesecke A, Rüdiger G and Elstner D 2005 *Astron. Nachr.* **326** 693–700 (*Preprint* astro-ph/0509286)
[40] Watson G N 1958 *A Treatise on the Theory of Bessel Functions* (Cambridge: Cambridge University Press)
[41] Luke Y L 1962 *Integrals of Bessel Functions* (New York: McGraw-Hill)